JHEP

Published for SISSA by Springer

Received: May 3, 2016
Accepted: July 18, 2016
Published: August 11, 2016

Minimal area surfaces dual to Wilson loops and the Mathieu equation

Changyu Huang, Yifei He and Martin Kruczenski

Department of Physics and Astronomy, Purdue University,
525 Northwestern Avenue, W. Lafayette, IN, 47907-2036 U.S.A.

E-mail: cyhuang@purdue.edu, he163@purdue.edu, markru@purdue.edu

Abstract: The AdS/CFT correspondence relates Wilson loops in $\mathcal{N} = 4$ SYM to minimal area surfaces in $AdS_5 \times S^5$ space. Recently, a new approach to study minimal area surfaces in $AdS_3 \subset AdS_5$ was discussed based on a Schroedinger equation with a periodic potential determined by the Schwarzian derivative of the shape of the Wilson loop. Here we use the Mathieu equation, a standard example of a periodic potential, to obtain a class of Wilson loops such that the area of the dual minimal area surface can be computed analytically in terms of eigenvalues of such equation. As opposed to previous examples, these minimal surfaces have an umbilical point (where the principal curvatures are equal) and are invariant under λ-deformations. In various limits they reduce to the single and multiple wound circular Wilson loop and to the regular light-like polygons studied by Alday and Maldacena. In this last limit, the periodic potential becomes a series of deep wells each related to a light-like segment. Small corrections are described by a tight-binding approximation. In the circular limit they are well approximated by an expansion developed by A. Dekel. In the particular case of no umbilical points they reduce to a previous solution proposed by J. Toledo. The construction works both in Euclidean and Minkowski signature of AdS_3.

Keywords: AdS-CFT Correspondence, Wilson, 't Hooft and Polyakov loops

ArXiv ePrint: 1604.00078

doi:10.1007/JHEP08(2016)088

JHEP08(2016)088

Contents

JHEP08(2016)088

1 Introduction

The AdS/CFT correspondence [1–3] is a duality between gauge theories and string theory. In the large N limit [4, 5] and at strong 't Hooft coupling the strings can be treated semi-classically. Since the classical solution of the string equations of motion is given by an extremal surface, the study of minimal area surfaces in AdS space is crucial in exploring the correspondence. In particular the relation between Wilson loops and minimal area surfaces ending at the boundary [6, 7] is an intense area of research [8–39]. In the case of single contour, smooth Wilson loops that interests us in this paper, analytical results for the minimal area problem are known in the case of near circular Wilson loop [40–43] based on perturbation theory, and for the case of surfaces with no umbilical points[1] [44–46] using Riemann theta functions along the lines of [47, 48] and a solution proposed by Toledo [49] using the Y-function method. For surfaces with umbilical points the only analytical results are for light-like Wilson loops with cusps [50–57]. An exception us the circular Wilson loop since the dual surface is a half-sphere and all points are umbillical (both curvatures equal).

[1] An umbilical point is a point where both principal curvatures coincide, in terms of the Pohlmeyer reduction described below it is a zero of the analytic function $f(z)$.

Finally let's point out that these developments are related to integrability properties of the sigma model that also appear in the closed string case [20, 58–66].

Going back to the minimal area problem, in this paper we concentrate in the case of Euclidean surfaces embedded in $EAdS_3$ and AdS_3 considered as subspaces of $AdS_5 \times S^5$. They are dual to space-like Wilson loops embedded in a subspace $\mathbb{R}^2 \subset \mathbb{R}^{3,1}$ or $\mathbb{R}^{1,1} \subset \mathbb{R}^{3,1}$. For concreteness, in the rest of the introduction we review the $EAdS_3$ case, the AdS_3 case is similar. A standard approach to the minimal area surface problem is to use the Pohlmeyer reduction [67]. First, the world-sheet is taken to be a unit disk and the induced metric is written in conformal coordinates $z = \sigma + i\tau$, namely in coordinates where it is conformally flat:

$$ds^2 = 4e^{2\alpha} dz d\bar{z}\,, \tag{1.1}$$

for some function $\alpha(z, \bar{z}) \in \mathbb{R}$. The crucial observation is that $\alpha(z, \bar{z})$ satisfies a generalized cosh-Gordon equation

$$\partial\bar{\partial}\alpha = e^{2\alpha} + f(z)\bar{f}(\bar{z})e^{-2\alpha}\,, \tag{1.2}$$

where $f(z)$ is a holomorphic function that depends on the shape of the Wilson loop. After solving this equation one can compute the regularized area by the formula

$$\mathcal{A}_f = -2\pi - 4\int_D f\bar{f}e^{-2\alpha} d\sigma d\tau\,, \tag{1.3}$$

where D represents the unit disk $|z| \leq 1$. This regularized area determines the expectation value of the corresponding Wilson loop in the field thepry at large 't Hooft coupling. When $f(z)$ has no zeros in the world-sheet, analytical solutions to the cosh-Gordon equation can be found using Riemann theta functions [44–46]. Alternatively, given a nowhere vanishing $f(z)$ one can solve a Y-system type of equation [49] and from there compute the area. In the case where $f(z)$ has zeros, the only known analytical results are for the Minkowski case and then only for Wilson loops with light-like boundaries [57].

In this paper we find analytical results for the case where $f(z) = f_0 z^n$, namely $f(z)$ has a multiple zero and the Wilson loop is given by a smooth space-like curve with no cusps. In order to do that, we use a way to approach the problem described in [68] where it was argued that such surfaces can be studied by considering a Schroedinger equation defined on the Wilson loop. Indeed, consider for concreteness the case of the Poincaré patch of $EAdS_3$ whose boundary is $\mathbb{R}^2$ and suppose that such Wilson loop is given by an arbitrary parameterization $X(s) = X_1(s) + iX_2(s)$, $s = 0 \ldots 2\pi$. Then one can define a Schroedinger equation

$$-\partial_s^2\chi + V(s)\chi(s) = 0\,, \tag{1.4}$$

where $V(s)$ is a complex potential given by

$$V(s) = V_0(s) + iV_1(s) = -\frac{1}{2}\{X(s), s\}\,, \tag{1.5}$$

where $\{X(s), s\}$ denotes the Schwarzian derivative. Up to global conformal transformations we can reconstruct the shape of the Wilson loop by considering two linearly independent

JHEP08(2016)088

solutions of such equation and taking the ratio

$$X(s) = \frac{\chi_1(s)}{\chi_2(s)}\,. \tag{1.6}$$

Such solutions are anti-periodic as can be seen from their explicit form:

$$\chi_1(s) = \frac{X(s)}{\sqrt{\partial_s X(s)}}, \qquad \chi_2 = \frac{1}{\sqrt{\partial_s X(s)}}\,. \tag{1.7}$$

The method proceeds by defining a generalized potential depending on a complex spectral parameter λ:

$$V(\lambda, s) = V_0(s) + \frac{i}{2}\left(\lambda + \frac{1}{\lambda}\right) V_1(s) + \frac{1}{2}\left(\lambda - \frac{1}{\lambda}\right) V_2(s)\,, \tag{1.8}$$

where $V_2(s)$ is such that the solutions of the corresponding Schroedinger equation are anti-periodic for any value of the parameter λ. Since the solutions of a Schroedinger equation with periodic potential are usually quasi-periodic, this provides an infinite set of condition that should be sufficient to determine the function $V_2(s)$. Once $V_2(s)$ is found the area follows from a simple formula. In this paper we used this method to find new Wilson loops whose shape and area can be computed analytically. The shape of the dual surface can then be obtained numerically.

2 Euclidean AdS_3 case

In this case we use Poincaré coordinates (X_1, X_2, Z) where $EAdS_3$ has a metric

$$ds^2 = \frac{dX_1^2 + dX_2^2 + dZ^2}{Z^2}\,. \tag{2.1}$$

The boundary is at $Z = 0$ and the Wilson loop is given by a curve

$$X(s) = X_1(s) + iX_2(s)\,. \tag{2.2}$$

where X is a complex coordinate. The world-sheet is parameterized by a complex coordinate $z = re^{i\theta}$, $|z| = r \leq 1$. The boundary conditions for the surface are that $Z(e^{i\theta}) = 0$ and $X(e^{i\theta}) = X(s(\theta))$ for some reparameterization $s(\theta)$. For every such curve, the minimal area problem leads to a particular function $f(z)$ and $\alpha(z, \bar{z})$ that satisfy eq. (1.2). If those functions are found then the minimal area can be computed using eq. (1.3). To find them, we can use the method proposed in [68] and summarized in the previous section. The functions $V_{0,1,2}(s)$ in eq. (1.8) are directly related to f and α [68]. When we choose $s = \theta$, the conformal angle as a parameter, the relation is given in eqs. (2.15), (2.18) below.

It is possible to implement a numerical approach to solve this problem. However, in this paper we find new analytical solutions by looking directly at the periodic Schroedinger equation. In fact, the prototypical periodic Schroedinger equation is the well-known Mathieu equation [69–71]:

$$\partial_u^2 \chi(u) + (a - 2q\cos 2u)\chi(u) = 0\,, \tag{2.3}$$

JHEP08(2016)088

where q is a parameter and a plays the role of energy eigenvalue. It has quasi-periodic solutions known as Floquet solutions

$$\chi_\nu(u+\pi) = e^{i\pi\nu}\chi_\nu(u)\,, \tag{2.4}$$

where the Mathieu characteristic $\nu = \nu(a,q)$ is a function of the parameters a and q. For given q we can fix ν to any desired value by choosing an appropriate value of $a = a_\nu(q)$. It is therefore natural to look for minimal area surfaces based on the Mathieu equation. In order to do that, we write the potential in eq. (1.8) as

$$V(\lambda,s) = -\frac{1}{4} + 6\beta_2 - \lambda f_0 e^{i(n+2)s} + f_0\frac{1}{\lambda}e^{-i(n+2)s}\,, \tag{2.5}$$

corresponding to the real and periodic functions

$$V_0(s) = -\frac{1}{4} + 6\beta_2, \qquad V_1(s) = -2f_0\sin(n+2)s, \qquad V_2(s) = -2f_0\cos(n+2)s\,. \tag{2.6}$$

The independent parameters are n, an even integer and f_0, a real constant. The constant β_2, however, is not arbitrary. The reason is that, if this potential corresponds to solutions of the minimal area problem, then the solutions to the corresponding Schroedinger equation should be anti-periodic for any value of λ. Consider the case when $\lambda = e^{i\varphi}$. It is clear that the potential is the same up to a shift in the variable s and therefore the periodicity of the solutions will be the same for any value of φ and, by analyticity, for any complex value of λ. Therefore we only need to ensure that the solutions are anti-periodic for $\lambda = 1$ which is easily done by choosing β_2 appropriately. Indeed, by defining

$$u(s) = \frac{(n+2)s+\varphi}{2} + \frac{\pi}{4}\,, \tag{2.7}$$

the equation

$$-\partial_s^2\chi(s) + V(\lambda,s)\chi(s) = 0\,, \tag{2.8}$$

becomes the standard Mathieu equation with

$$a = \frac{1-24\beta_2}{(n+2)^2}, \qquad q = \frac{4if_0}{(n+2)^2}\,. \tag{2.9}$$

Now we look for a Floquet solution of Mathieu equation with real characteristic exponent ν, i.e.

$$\chi_\nu(u+\pi) = e^{\pi i\nu}\chi_\nu(u)\,, \tag{2.10}$$

or equivalently

$$\chi_\nu(u) = e^{i\nu u}\,p_\nu(q,u)\,, \tag{2.11}$$

where $p_\nu(\theta)$ is π periodic. Since we require $\chi(s)$ to be an anti-periodic function of $s = 0\ldots 2\pi$, it follows that, when $\Delta s = 2\pi$,

$$\begin{aligned} \Delta u &= (n+2)\pi\,, \\ (2k+1)\pi = \nu\Delta u\,, \qquad &\Rightarrow \qquad \nu = \frac{2k+1}{n+2} \qquad (k\in\mathbb{Z})\,, \end{aligned} \tag{2.12}$$

Thus there is a discrete family of solutions labeled by $k \in \mathbb{Z}$. Such solutions, however do not necessarily have one boundary. Later we will see that for $k = 0$ they do (and also, in certain cases, for $k = n + 1$). For each ν the Mathieu eigenvalue $a = a_\nu(q)$ can be determined[2] and from there the constant

$$\beta_2 = \frac{1}{24}\left[1 - (n+2)^2 a_\nu(q)\right] , \tag{2.13}$$

that, as seen in the next section, gives the area of the minimal surface. The shape of the Wilson loop is given by the ratio of two independent solutions of the Mathieu equation

$$X(u) = \frac{\chi_\nu(u)}{\chi_\nu(-u)} = e^{2i\nu u}\,\frac{p_\nu(q,u)}{p_\nu(q,-u)} = \frac{Mc(u) + iMs(u)}{Mc(u) - iMs(u)} , \tag{2.14}$$

where we used that replacing $u \to -u$ gives another solution of the Mathieu equation. For completeness, we also wrote the result in terms of the often used Mathieu sine and cosine defined as the odd and even solutions respectively. All Mathieu functions are evaluated for q given in eq. (2.9) and the eigenvalue $a = a_\nu(q)$.

At this point it is useful to make contact with the Pohlmeyer reduction method. Indeed, from [68], the potential is given by

$$V(\theta) = -\frac{1}{4} + 6\beta_2(\theta) - f(\theta)\lambda e^{2i\theta} + \frac{1}{\lambda} e^{-2i\theta}\bar{f}(\theta) , \tag{2.15}$$

which means that, if we identify $s = \theta$, these solutions correspond to a holomorphic function

$$f(z) = f_0 z^n , \tag{2.16}$$

which has no poles inside the disk, therefore justifying the choice $s = \theta$. The function $\beta_2(\theta)$ is constant and given by eq. (2.13). Replacing in the generalized cosh-Gordon equation (1.2), one can see that the equation is solved by a rotationally invariant function $\alpha(r)$ satisfying

$$\partial_r^2 \alpha(r) + \frac{1}{r}\partial_r \alpha(r) = 4e^{2\alpha(r)} + 4f_0^2 r^{2n} e^{-2\alpha(r)} . \tag{2.17}$$

Near the boundary $r \to 1$ this equation implies that, in terms of the variable $\xi = 1 - r^2$,

$$\alpha = -\ln\xi + \beta_2\xi^2 + \beta_2\xi^3 + \mathcal{O}(\xi^4), \qquad (\xi = 1 - r^2 \to 0) , \tag{2.18}$$

as already derived in [68] but with the observation that here β_2 is a constant independent of θ. In the Minkowski case, such function $f(z) = f_0 z^n$ was studied by Alday and Maldacena [72][3] where it was noticed that eq. (2.17) is equivalent to the Painleve III equation. However only the case of an infinite world-sheet was considered, corresponding to a light-like Wilson loop with cusps. For the case of smooth Wilson, loops J. Toledo recently found one such example of solution using his Y-system method [49]. Here it corresponds to the case $n = 0$ where $f(z)$ does not vanish anywhere on the world-sheet. On the other hand

[2] There are efficient numerical algorithms to obtain the eigenvalues, for example Mathematica implements such function $a_\nu(q)$.

[3] They were called "regular polygon" solutions.

JHEP08(2016)088

the solutions presented here correspond to the case of smooth Wilson loops where $f(z)$ has zeros, a case where no exact results for the area were known before. This equation was also studied in [73] in relation to minimal area surfaces but the surfaces considered there were different (multiple boundaries) and the area was not computed. Nevertheless, those results have some overlap with the Euclidean case considered in this paper.

3 Computation of the area

To compute the area we can use simple integration by parts in eq. (1.3). In order to do that we observe that eq. (2.17) implies that

$$\partial_r \left[r^2(\partial_r\alpha)^2 + 2r\partial_r\alpha - 4r^2e^{2\alpha} + 4f_0^2 r^{2n+2} e^{-2\alpha} \right] = 8(n+2) f_0^2 r^{2n+1}\, e^{-2\alpha}\,. \tag{3.1}$$

Thus

$$\begin{aligned} \mathcal{A}_f + 2\pi &= -4\int_D f\bar{f} e^{-2\alpha}\, r dr\, d\theta = -8\pi f_0^2 \int_0^1 r^{2n+1} e^{-2\alpha(r)}\, dr \\ &= -\frac{\pi}{n+2}\int_0^1 \partial_r \left[r^2(\partial_r\alpha)^2 + 2r\partial_r\alpha - 4r^2e^{2\alpha} + 4f_0^2 r^{2n+2} e^{-2\alpha} \right] dr \\ &= \frac{-\pi}{(n+2)} \left[r^2(\partial_r\alpha)^2 + 2r\partial_r\alpha - 4r^2e^{2\alpha} \right]\Big|_{r\to 1} \\ &= \frac{24\pi\beta_2}{n+2}\,, \end{aligned} \tag{3.2}$$

where we used the behavior (2.18) for α at the world-sheet boundary. In this case $\beta_2 < 0$ implying that $\mathcal{A}_f < -2\pi$. Finally, using eq. (2.13), the area can be put in terms of the eigenvalues $a_\nu(q)$ of the Mathieu equation

$$\mathcal{A}_f = -2\pi + \frac{\pi}{n+2} - (n+2)\pi a_\nu(q)\,. \tag{3.3}$$

This concludes the computation of the area. However it is important to point out that the fact that the integrand in (1.3) is a total derivative is not a coincidence but quite generic. Indeed, in [68] and [74], using integration by parts, a formula for the area in terms for the Schwarzian derivative of the contour was given. It is valid whenever $f(z)$ has no zeros on the world-sheet, clearly not the case here since $f(z) = f_0 z^n$. The problem in using the formula is that, when $f(z)$ has zeros, the function $\sqrt{f}$ has cuts and the integration by parts in eq. (111) of [74] gives rise to integrals around the cuts as in [57]. However, in the present case, when n is even the function $\sqrt{f}$ is well-defined, thus we can define the function

$$W(z) = \int_0^z \sqrt{f(z')} dz' = \frac{2\sqrt{f_0}}{n+2}\, z^{\frac{n}{2}+1}\,, \tag{3.4}$$

JHEP08(2016)088

and use the same argument as in [74]. It starts with the observation that the generalized cosh-Gordon equation implies

$$\begin{aligned} j &= j_z dz + j_{\bar{z}} d\bar{z}\,, \\ j_z &= 4f\sqrt{\bar{f}}e^{-2\alpha}\,, \\ j_{\bar{z}} &= \frac{2}{\sqrt{\bar{f}}}\left[\bar{\partial}^2\alpha - (\bar{\partial}\alpha)^2\right]\,, \\ dj &= 0\,, \end{aligned} \tag{3.5}$$

and therefore

$$\begin{aligned} \mathcal{A}_f + 2\pi &= -4\int_D f\bar{f}e^{-2\alpha}d\sigma d\tau \\ &= -\frac{i}{2}\int_D j\wedge d\bar{W} = \frac{i}{2}\int_D d(\bar{W}j) \\ &= \frac{i}{2}\oint_{\partial D}\bar{W}(j_z\,dz + j_{\bar{z}}\,d\bar{z})\,. \end{aligned} \tag{3.6}$$

A caveat is that in [74] the component $j_{\bar{z}}$ was defined with an extra $\{\bar{W},\bar{z}\}$ so that j transforms properly as a one form. Here this is not possible since $\{W,z\}$ has a double pole at zero and therefore it would give an extra contribution to the contour integral. Continuing the reasoning along the lines of [74], the boundary behavior of $j_{\bar{z}}$ is given by

$$j_{\bar{z}} = \frac{1}{\sqrt{\bar{f}}}(12\beta_2(\theta)e^{2i\theta}) + \mathcal{O}(\xi) \qquad (\xi = 1 - r^2 \to 0)\,, \tag{3.7}$$

whereas $j_z \to 0$ and therefore

$$\mathcal{A}_f = -2\pi + \frac{i}{2}\oint_D \frac{\bar{W}}{\sqrt{\bar{f}}}12\beta_2 e^{2i\theta}\partial_\theta\bar{z}\,d\theta\,. \tag{3.8}$$

Replacing $W(z)$ from eq. (3.4), $f = f_0 z^n$ and $z = e^{i\theta}$ it follows that

$$\mathcal{A}_f = -2\pi + \frac{24\pi\beta_2}{n+2}\,, \tag{3.9}$$

in perfect agreement with eq. (3.2).

4 Numerical checks, examples and limits of the solutions

The previous sections give analytic results for the shape of the Wilson loop (boundary curve) and for the area of the dual minimal area surface. It does not however give an analytic expression for the shape of the surface. In this section we use a numerical procedure to independently find these solutions (including the shape of the minimal surface) providing a numerical test of the previous results. In order to do so we first solve numerically the generalized cosh-Gordon equation for α, eq. (1.2) and then the linear problem [68] for $\psi_{1,2}$ that leads to the shape of the surface and boundary contour. Finally, the integral in eq. (1.3) can be done numerically providing a check of the previous results.

JHEP08(2016)088

With the choice $f = f_0 z^n$, $f_0 \in \mathbb{R}$, the generalized cosh-Gordon equation reads

$$\partial\bar{\partial}\alpha = e^{2\alpha} + f_0^2 |z|^{2n} e^{-2\alpha}\,, \tag{4.1}$$

and therefore has solutions that depend only on the radial coordinate $\alpha(r)$ where $z = re^{i\theta}$. In this case the equation becomes

$$\frac{1}{4}\left[\partial_r^2\alpha + \frac{1}{r}\partial_r\alpha\right] = e^{2\alpha} + f_0^2 r^{2n} e^{-2\alpha}\,. \tag{4.2}$$

For numerical purposes, it is convenient to define r_0 such that $f_0 = r_0^{n+2}$ and then rescale $r = \frac{\tilde{r}}{r_0}$ and introduce $\tilde{\alpha} = \alpha - \ln r_0$ so that the equation becomes

$$\frac{1}{4}\left[\partial_{\tilde{r}}^2\tilde{\alpha} + \frac{1}{\tilde{r}}\partial_{\tilde{r}}\tilde{\alpha}\right] = e^{2\tilde{\alpha}} + \tilde{r}^{2n} e^{-2\tilde{\alpha}}\,. \tag{4.3}$$

Now we choose a value of $\tilde{\alpha}(\tilde{r}=0) = \tilde{\alpha}_0$ and, using the boundary condition $\partial_{\tilde{r}}\tilde{\alpha}|_{\tilde{r}=0} = 0$, integrate the differential equation up to a value $\tilde{r} = r_0$ where $\tilde{\alpha}$ diverges. This allows us to find $r_0(\tilde{\alpha}_0)$, namely for numerical purposes $\tilde{\alpha}_0$ is the parameter that defines the solution and f_0 is derived. To reconstruct the surface we now use the formulas (and notation) of [68]. First the linear problem

$$\partial_{\tilde{r}}\psi_1 = \left(e^{i\theta+\tilde{\alpha}} - \tilde{r}^n e^{-\tilde{\alpha}-i(n+1)\theta}\right)\psi_2\,, \tag{4.4}$$

$$\partial_{\tilde{r}}\psi_2 = \left(e^{-i\theta+\tilde{\alpha}} + \tilde{r}^n e^{-\tilde{\alpha}+i(n+1)\theta}\right)\psi_1\,, \tag{4.5}$$

is easily solved numerically[4] and the shape of the surface reconstructed by first taking two linearly independent solutions (ψ_1, ψ_2), $(\tilde{\psi}_1, \tilde{\psi}_2)$. For example by using the initial conditions, $(\psi_1(0) = 1, \psi_2(0) = 0)$ and $(\tilde{\psi}_1(0) = 0, \tilde{\psi}_2 = 1)$. With those soltions, the following matrices can be constructed:

$$\mathbb{A} = \begin{pmatrix} \psi_1 & \psi_2 \\ \tilde{\psi}_1 & \tilde{\psi}_2 \end{pmatrix}, \qquad \mathbb{X} = \mathbb{A}.\mathbb{A}^\dagger\,. \tag{4.6}$$

The Poincaré coordinates are identified, in terms of the components of $\mathbb{X}$ as

$$Z = \frac{1}{\mathbb{X}_{22}}, \qquad X = X_1 + iX_2 = \frac{\mathbb{X}_{21}}{\mathbb{X}_{22}}\,. \tag{4.7}$$

This method is rather crude and can be much improved by solving the equation using series expansions around $\tilde{r} = 0$ and $\tilde{r} = r_0$ and then matching the expansions at some intermediate point to determine the function $r_0(\tilde{\alpha}_0)$. For example for $n = 2$ the expansions read

$$\tilde{\alpha} = \tilde{\alpha}_0 + e^{2\,\tilde{\alpha}_0}\tilde{r}^2 + \frac{1}{2}e^{4\,\tilde{\alpha}_0}\tilde{r}^4 + \left(\frac{e^{6\,\tilde{\alpha}_0}}{3} + \frac{e^{-2\,\tilde{\alpha}_0}}{9}\right)\tilde{r}^6 + \dots\,, \tag{4.8}$$

$$\tilde{\alpha} = -\ln r_0 - \ln\xi + \beta_2\,\xi^2 + \beta_2\,\xi^3 + \frac{1}{10}\left(r_0^{20} + 2\beta_2^2 + 9\beta_2\right)\xi^4 + \dots\,, \tag{4.9}$$

where $\xi = 1 - \frac{\tilde{r}^2}{r_0^2}$. The resulting shapes and values for the area match perfectly the results obtained from the Mathieu equation. To get an idea of the shape we present some typical results in figure 1.

[4] Numerically, eq. (4.3) and the linear problem are solved simultaneously.

JHEP08(2016)088

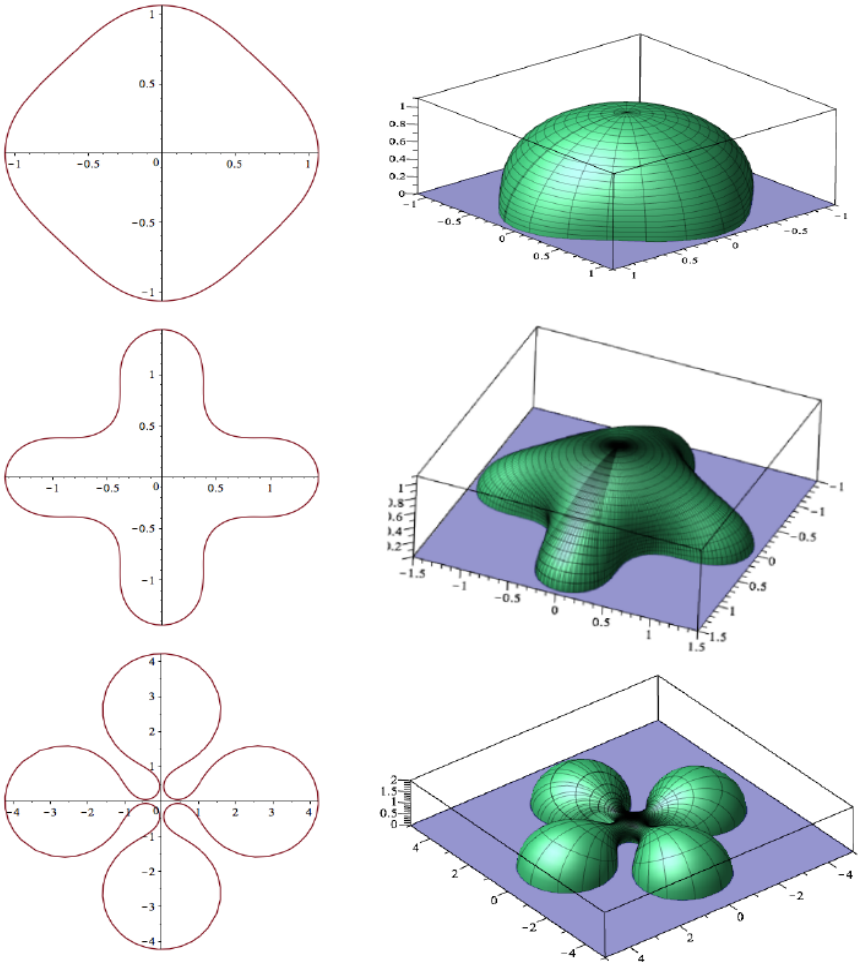

Figure 1. Surface corresponding to $n = 2$ and the parameters $[\tilde{\alpha}_0, r_0, \beta_2, \mathcal{A}_f]$ equal to (top to bottom): $[0.01, 0.986067, -0.0200117, -6.660397]$, $[-.45, 1.4164114, -.43083877, -14.404305]$, $[-.95, 1.5079094, -1.3248754, -31.2565]$.

4.1 Limits

Further, to get a better understanding of the solutions we consider several values of n and swipe the values of $\tilde{\alpha}_0$ from minus to plus infinity. In the limit $\tilde{\alpha}_0 \to \infty$ the exponential term $e^{-2\alpha}$ in the cosh-Gordon equation (4.1) becomes negligible and the solution approaches the one with $f(z) = 0$, namely the circular Wilson loop. In the Mathieu equation $q \to 0$ and we can use standard techniques to approximate the solutions as deformations of the circle (see appendix). For finite values of $\tilde{\alpha}_0$ the Wilson loop resembles a smoothed out regular polygon with $n + 2$ sides. As $\tilde{\alpha}_0$ decreases, the shape of the Wilson loop changes until at a certain value there is a discontinuity where the Mathieu characteristic $\nu(a, q)$ jumps from $\nu = \frac{1}{n+2}$ to $\nu = 2 - \frac{1}{n+2}$ and the Wilson loops becomes multiple wound. In the limit $\tilde{\alpha}_0 \to -\infty$ it becomes a multiple wound circle, the winding number is $k = 2n + 3$. The constant β_2 takes the value $\beta_2 = -\frac{1}{6}(n + 1)(n + 2)$ and the area is $\mathcal{A}_f = -2(2n + 3)\pi$.

Finally it is also worth mentioning the limit $n \to \infty$ in which case the function r^{2n} vanishes in the relevant region ($r < 1$). In this case the solution approaches the circular Wilson loop.

JHEP08(2016)088

4.2 Relation to Painleve III equation

We conclude this section by mentioning that, as noted in [73] for the Euclidean and [72] for the Minkowski case, the radial cosh/sinh-Gordon equation is equivalent to the Painleve III equation. Indeed, the change of variables

$$\begin{aligned} y &= \frac{1}{f_0}\frac{1}{r^n}e^{2\alpha}\,, \\ t &= r^{n+2}\,, \end{aligned} \tag{4.10}$$

reduces eq. (4.2) to the standard form

$$\frac{y^2}{t}\left(\frac{d}{d\ln t}\right)^2(\ln y) = tyy'' + yy' - t(y')^2 = by + ay^3 + t(\delta + \gamma y^4)\,, \tag{4.11}$$

with parameters

$$b = a = \frac{8f_0}{(n+2)^2} = -2iq, \qquad \delta = \gamma = 0\,. \tag{4.12}$$

The function $y(t)$ has a singularity at $t = 1$ corresponding to $r = 1$ namely the world-sheet boundary. Using the expansion (2.18) and after the change of variables (4.10) it follow that

$$y(t) = \frac{i}{q}\frac{1}{(1-t)^2} + \frac{i}{12}\frac{1-4a_\nu(q)}{q}(1+(1-t)) + \mathcal{O}[(1-t)^2]\,, \tag{4.13}$$

namely, the solution $y(t)$ that has a double pole singularity at $t = 1$ and the constant and linear coefficients in the Laurent expansion are determined by the eigenvalues $a_\nu(q)$ of the Mathieu equation. This provides an interesting relation between the Painleve III and Mathieu equation, namely that the Mathieu eigenvalues control the behavior near the movable singularity [73].

5 Comparison with wavy-line approximation

In the limit $f_0 \to 0$ the solutions approach the circular Wilson loop. In the Mathieu equation this corresponds to the limit $q \to 0$ that can be studied by standard perturbative methods. In this section, however we employ the method developed by A. Dekel in [43] to study an arbitrary near circular Wilson loop providing then a check of that method. The idea is to assume that the contour has the shape given by the ratio of Mathieu functions in eq. (2.14), expand it for small q and use Dekel's method to compute the area and check the result by comparing with eq. (3.3). We start by parameterizing the contour as a perturbation of a circular Wilson loop:

$$X(\theta) = e^{i\,s(\theta)+\xi(s(\theta))}\,. \tag{5.1}$$

Here $s(\theta)$ is the correct parametrization which we assume is unknown, and $\xi(s)$ to the third order of the perturbation takes the form (see appendix)

$$\xi(s) = a(-iq)\sin\left(\frac{s}{\nu}\right) + (-iq)^3\left(b\sin\left(\frac{s}{\nu}\right) + c\sin\left(\frac{3s}{\nu}\right)\right)\,, \tag{5.2}$$

JHEP08(2016)088

with

$$
\begin{aligned}
a &= \frac{\nu}{\nu^2-1}, \\
b &= -\frac{3\nu\left(\nu^2+5\right)}{16\left(\nu^2-4\right)\left(\nu^2-1\right)^3}, \\
c &= -\frac{\nu\left(5\nu^4+36\nu^2-89\right)}{48\left(\nu^2-9\right)\left(\nu^2-4\right)\left(\nu^2-1\right)^3}.
\end{aligned}
\tag{5.3}
$$

If we let $\epsilon = -iq$, $p = \frac{1}{\nu}$, then the contour becomes

$$
X(\theta) = e^{is(\theta)+\epsilon a \sin(ps(\theta))+\epsilon^3(b\sin(ps(\theta))+c\sin(3ps(\theta)))}. \tag{5.4}
$$

With such parametrization, we can use the method introduced by Dekel in [43] for the area calculation of the minimal surface ending on $X(\theta)$. Here we briefly review the procedure.

The expression for the regularized area is given in eq. (1.3). Therefore, we need to have $f(z)$ and solve the generalized cosh-Gordon equation for $\alpha(z,\bar{z})$ to calculate the area. These functions can be expanded as

$$
\begin{aligned}
f(z) &= \sum_{n=1}^{\infty} f_n(z)\epsilon^n, \\
\alpha(z,\bar{z}) &= \ln\left(\frac{1}{1-z\bar{z}}\right) + \sum_{n=2}^{\infty}\alpha_n(z,\bar{z})\epsilon^n.
\end{aligned}
\tag{5.5}
$$

Meanwhile, the correct parametrization $s(\theta)$ has the expansion

$$
s(\theta) = s(\theta) = \theta + \sum_{n=1}^{\infty} s_n(\theta)\epsilon^n. \tag{5.6}
$$

When $\epsilon = 0$, $X(\theta)$, $s(\theta)$, $f(z)$ and $\alpha(z,\bar{z})$ reduce to the results of circular Wilson loop. From the given boundary contour $X(s(\theta))$ we can first calculate the real and imaginary parts of the Schwarzian derivative expressed with the unknown $s_n(\theta)$. Based on the relations [68]

$$
\begin{aligned}
\mathrm{Re}\{X(\theta),\theta\} &= \frac{1}{2} - 12\beta_2(\theta), \\
\mathrm{Im}\{X(\theta),\theta\} &= -4\,\mathrm{Im}(e^{2i\theta}f(\theta)),
\end{aligned}
\tag{5.7}
$$

we then expand the l.h.s. of the equations with the parameter ϵ and extract $f(\theta)$ and $\beta_2(\theta)$ order by order. Next we plug $f(z)$ into the generalized cosh-Gordon equation to solve for $\alpha(z,\bar{z})$ and expand the solution around $r = 1$ to get $\beta_2(\theta)$ which we use to compare with (5.7) to fix $s_n(\theta)$. In the end, we plug $s_n(\theta)$ back into $f(z)$, $\alpha(z,\bar{z})$ and (1.3) to get the area.

As it turns out, the term $c\sin(3p\,s(\theta))$ in the contour parametrization given in eq. (5.2) appears in the area only at order ϵ^6 and higher. Besides, to order ϵ^4, the $b\sin(p\,s(\theta))$ term appears in the area expression as a first order effect, i.e., if we parametrize the contour as

$$
X(\theta) = e^{is(\theta)+\epsilon a'\sin(p\,s(\theta))+O(\epsilon^3)}, \tag{5.8}
$$

JHEP08(2016)088

and let $a' = a + b\epsilon^2$, the area calculation will give the same result as the one given by (5.2) to order ϵ^4. Since we are comparing the area with the one given by Mathieu function only to the fourth order of the perturbation, we will adopt the parametrization (5.8) and make the replacement

$$a' = \frac{\nu}{\nu^2 - 1} + \frac{3\nu\left(\nu^2 + 5\right) q^2}{16\left(\nu^2 - 4\right)\left(\nu^2 - 1\right)^3}\,, \tag{5.9}$$

at the end.

Our calculation shows that the expansions of the functions have the following form

$$\begin{aligned}
s(\theta) &= \theta - \frac{a'^2(p + 5p^3)\sin(2p\theta)}{8(-1 + 4p^2)}\epsilon^2 + O(\epsilon^4)\,,\\
f(z) &= -\frac{1}{4}ia'p\left(p^2 - 1\right)z^{p-2}\epsilon + \frac{3ia'^3p^3\left(p^2 - 1\right)\left(5p^2 + 1\right)z^{p-2}}{64\left(4p^2 - 1\right)}\epsilon^3 + O(\epsilon^4)\,,\\
\alpha(r,\theta) &= \ln\left(\frac{1}{1 - r^2}\right) + \frac{a'^2p}{16r^2\left(r^2 - 1\right)}(4r^2 + 4r^4 - p(p+1)^2r^{2p}\\
&\quad + (p+1)^2(3p - 4)r^{2p+2} - (p-1)^2(3p+4)r^{2p+4} + (p-1)^2pr^{2p+6})\epsilon^2\\
&\quad + O(\epsilon^4)\,.
\end{aligned} \tag{5.10}$$

Finally, the area is given by:

$$\mathcal{A}_f = -2\pi - \frac{1}{2}p\left(p^2 - 1\right)\pi a'^2\epsilon^2 + \frac{p\left(p^2 - 1\right)\left(23p^4 + p^2\right)\pi a'^4}{32\left(4p^2 - 1\right)}\epsilon^4 + O(\epsilon^5)\,. \tag{5.11}$$

Plugging (5.9) into (5.11), and setting $\epsilon = -iq$, $p = \frac{1}{\nu}$, the area is given by

$$\mathcal{A}_f = -2\pi + \frac{\pi q^2}{2\nu(1 - \nu^2)} - \frac{\left(5\nu^2 + 7\right)\pi q^4}{32\nu\left(4 - \nu^2\right)\left(1 - \nu^2\right)^3} + O(q^6)\,. \tag{5.12}$$

This result agrees with the one we got from the Mathieu function calculation described in the appendix (see eq. (A.11)). Notice that, from eq. (2.9), q is purely imaginary and therefore $\mathcal{A}_f < -2\pi$ (since $\nu = \frac{1}{n+2} < 1$).

6 Minkowski case

It is interesting to consider the case of Minkowski signature since in that case the Wilson loops that we consider approach, in a limit, those used by Alday and Maldacena to compute scattering amplitudes [72, 75]. On the other hand, the methods we employ are similar to the Euclidean case. In Lorentzian signature, in Poincaré coordinates (T, X, Z) the metric of AdS_3 is

$$ds^2 = \frac{-dT^2 + dX^2 + dZ^2}{Z^2}\,. \tag{6.1}$$

The Wilson loop is given by a curve

$$x_+(s) = X(s) + T(s), \qquad x_-(s) = X(s) - T(s)\,. \tag{6.2}$$

JHEP08(2016)088

The light-cone coordinates $x_\pm \in \mathbb{R}$ are introduced for convenience. However it turns out to be even more convenient to use a conformal transformation and define complex coordinates

$$\hat{x}_\pm = \mp i \frac{1 \pm i x_\pm}{1 \mp i x_\pm}\,, \tag{6.3}$$

with the property $|\hat{x}_\pm| = 1$. Besides Poincaré coordinates it is also useful to use global coordinates (t, ϕ, ρ) such that the metric is

$$ds^2 = -\cosh^2\rho\, dt^2 + d\rho^2 + \sinh^2\rho\, d\phi^2\,. \tag{6.4}$$

The relation to Poincaré coordinates is better written using embedding coordinates (X_{-1}, X_0, X_1, X_2) satisfying $X_{-1}^2 + X_0^2 - X_1^2 - X_2^2 = 1$ and related to the previous coordinates by

$$Z = \frac{1}{X_{-1} - X_2}\,, \qquad X = \frac{X_1}{X_{-1} - X_2}\,, \qquad T = \frac{X_0}{X_{-1} - X_2}\,, \tag{6.5}$$

with the AdS_3 boundary located at $Z = 0$ while the global coordinates are defined as

$$X_{-1} + iX_0 = \cosh\rho\, e^{it}\,, \qquad X_1 + iX_2 = \sinh\rho\, e^{i\phi}\,, \tag{6.6}$$

with the boundary at $\rho \to \infty$. The boundary contour is given by a curve $(t(s), \phi(s))$ and is related to the coordinates $\hat{x}_\pm$ by

$$\hat{x}_\pm = e^{i(t \pm \phi)}\,. \tag{6.7}$$

Now we use the method described in [68] for the Euclidean case and generalized in [74] for the Minkowski case. In this case the Schroedinger equation associated with the Wilson loop shape reads [74]

$$\begin{aligned} -\partial_\theta^2 \chi(\theta) + V_\lambda(\theta)\chi(\theta) &= 0\,, \\ V_\lambda(\theta) &= -\frac{1}{4} + 6\beta_2(\theta) + \frac{1}{\lambda} i f(e^{i\theta}) e^{2i\theta} - \lambda i \bar{f}(e^{-i\theta}) e^{-2i\theta}\,. \end{aligned} \tag{6.8}$$

Given two linearly independent solutions $\chi_{1,2}^\lambda$ the shape of the boundary curve is determined as

$$\hat{x}_\pm = \frac{\chi_1^{\lambda=\pm 1}}{\chi_2^{\lambda=\pm 1}}\,. \tag{6.9}$$

The solutions $\chi_{1,2}^\lambda$ should be chosen such that $|\hat{x}_\pm| = 1$. Equivalently we can chose real solutions $\tilde{\chi}_{1,2}^\lambda$ and define the boundary shape as $x_\pm = \frac{\tilde{\chi}_1^{\lambda=\pm 1}}{\tilde{\chi}_2^{\lambda=\pm 1}}$.

In the case $f(z) = f_0 z^n$, and after taking $\lambda = e^{i\varphi}$ and defining a new coordinate

$$u = \frac{(n+2)\theta - \varphi}{2} + \frac{\pi}{4}\,, \tag{6.10}$$

we obtain a Mathieu equation with parameters

$$a = \frac{1 - 24\beta_2}{(n+2)^2}\,, \qquad q = \frac{4 f_0}{(n+2)^2}\,. \tag{6.11}$$

JHEP08(2016)088

The construction requires the solutions $\chi_{1,2}$ to be anti-periodic. We can then write them in terms of Floquet solutions

$$\chi_\nu(u+\pi) = e^{i\nu\pi}\chi_\nu(u)\,, \qquad \nu = \frac{2k+1}{n+2} \qquad (k \in Z)\,. \tag{6.12}$$

Noting that the parameters (a, q) in eq. (6.11) are real, the conjugate of a Floquet solution is another Floquet solution. Further, $u \to u + \frac{\pi}{2}$ is equivalent to replacing $\lambda \to -\lambda$, thus, the shape of the Wilson loop can be written as

$$\hat{x}_+ = \frac{\chi_\nu(u)}{(\chi_\nu(u))^*}\,, \tag{6.13}$$

$$\hat{x}_- = \frac{\left(\chi_\nu\left(u+\frac{\pi}{2}\right)\right)^*}{\chi_\nu\left(u+\frac{\pi}{2}\right)}\,, \tag{6.14}$$

which evidently satisfy $|\hat{x}_\pm| = 1$. Now, for a given value of ν we find the corresponding value $a_\nu(q)$ and the constant β_2 in eq. (6.8) follows as

$$\beta_2 = -\frac{1}{24}\left[1-(n+2)^2 a_\nu(q)\right]\,. \tag{6.15}$$

The area of the minimal surface ending on the boundary curve can be computed, as before, using integration by parts and results in

$$\mathcal{A}_f = -2\pi + 4\int_D f\bar{f}e^{-2\alpha}d\sigma d\tau \tag{6.16}$$

$$= -2\pi + \frac{24\pi\beta_2}{n+2} \tag{6.17}$$

$$= -2\pi - \frac{\pi}{n+2} + \pi(n+2)a_\nu(q)\,, \tag{6.18}$$

giving again an analytical formula for the area in terms of the eigenvalues of the Mathieu equation. Although the formula is the same as for the Euclidean case, now $\beta_2 > 0$ and the area is $\mathcal{A}_f > -2\pi$.

6.1 Numerics, examples and limits

As in the Euclidean case it is useful to plot the resulting surfaces to understand their behavior. To obtain the surface we refer to [74] for the derivations and we just present here the summary of steps necessary to obtain the shapes. As a first step we solve the generalized sinh-Gordon equation

$$\partial\bar{\partial}\alpha = e^{2\alpha} - f(z)\bar{f}(\bar{z})e^{-2\alpha}\,, \tag{6.19}$$

that again, for $f = f_0\, z^n$ has radial solutions obeying

$$\frac{1}{4}\left[\partial_r^2\alpha + \frac{1}{r}\partial_r\alpha\right] = e^{2\alpha} - f_0^2 r^{2n}e^{-2\alpha}\,. \tag{6.20}$$

Defining r_0 such that $f_0 = r_0^{n+2}$ and doing the same rescalings as done to arrive at (4.3) we obtain

$$\frac{1}{4}\left[\partial_{\tilde{r}}^2\tilde{\alpha} + \frac{1}{\tilde{r}}\partial_{\tilde{r}}\tilde{\alpha}\right] = e^{2\tilde{\alpha}} - \tilde{r}^{2n}e^{-2\tilde{\alpha}}\,. \tag{6.21}$$

We then look for solutions with given value of $\tilde{\alpha}(0)$ and $\partial_{\tilde{r}}\tilde{\alpha}|_{\tilde{r}=0} = 0$. After that, the linear problem

$$\partial_{\tilde{r}}\psi_1 = \left(\lambda e^{i\theta+\tilde{\alpha}} + \tilde{r}^n e^{-\tilde{\alpha}-i(n+1)\theta}\right)\psi_2\,, \tag{6.22}$$

$$\partial_{\tilde{r}}\psi_2 = \left(\frac{1}{\lambda}e^{-i\theta+\tilde{\alpha}} + \tilde{r}^n e^{-\tilde{\alpha}+i(n+1)\theta}\right)\psi_1\,, \tag{6.23}$$

needs to be solved for $\lambda = 1$ and $\lambda = -1$. Given the initial value $\tilde{\alpha}(0) = \alpha_0$, two linearly independent solutions can be found using, for example the initial conditions, $(\psi_1^\lambda(0) = 1, \psi_2^\lambda(0) = -i)$ and $(\tilde{\psi}_1^\lambda(0) = i, \tilde{\psi}_2^\lambda = -1)$.

Finally we can reconstruct the shape of the solutions through

$$\mathbb{A}^\lambda = \begin{pmatrix} \psi_1^\lambda & \psi_2^\lambda \\ \tilde{\psi}_1^\lambda & \tilde{\psi}_2^\lambda \end{pmatrix}\,, \qquad \mathbb{X} = R_M^{-1}\mathbb{A}^{\lambda=1}\left[\mathbb{A}^{\lambda=-1}\right]^{-1}R_M\,, \tag{6.24}$$

where R_M is a 2×2 matrix given by

$$R_M = \frac{1}{\sqrt{2}}\left(\mathbb{I} + i\sigma_1\right), \qquad \sigma_1 = \begin{pmatrix} 0 & 1 \\ 1 & 0 \end{pmatrix}\,. \tag{6.25}$$

Finally, the global coordinates follow as

$$t = \arg(-\mathbb{X}_{11}), \qquad \phi = \arg(\mathbb{X}_{12}), \qquad \tanh\rho = \left|\frac{\mathbb{X}_{12}}{\mathbb{X}_{11}}\right|\,. \tag{6.26}$$

Sweeping the possible values of $\tilde{\alpha}(0)$ we find that, when $\tilde{\alpha}(0) \to \infty$, the parameter q in the Mathieu equation vanishes and the solution becomes the circular solution $t = 0, \phi = \theta$, $(0 < \theta < 2\pi)$. As we lower $\tilde{\alpha}(0)$, the circle starts deforming and takes the shape seen in figure 2, seemingly a regularized version of a succession of light-like cusps. For a certain value of $\tilde{\alpha}(0)$, the parameter $q \to \infty$ and the Wilson loop becomes a series of light-like segments with the shape of the so called "regular polygons" considered in [72]. It has $2(n+2)$ light-like cusps, the particular case $n = 0$ has four light-like cusps and was first described in [50], eq. (71). For lower values of $\tilde{\alpha}(0)$, the solution no longer touches the boundary, it still ends in light like-lines but inside AdS. This can be seen in the last figure in figure 2. It will be interesting to understand the physical meaning of such solutions. The particular limits, $q \to 0$ and $q \to \infty$ are studied in the following subsections.

6.2 Near circular ($q \to 0$ approximation)

In the near circular case, we can use a simple generalization of Dekel's procedure from Euclidean to Lorentzian signature to compute the expansion in q. It is interesting that it also works in this case. From the point of view of the Mathieu functions, the expansion

JHEP08(2016)088

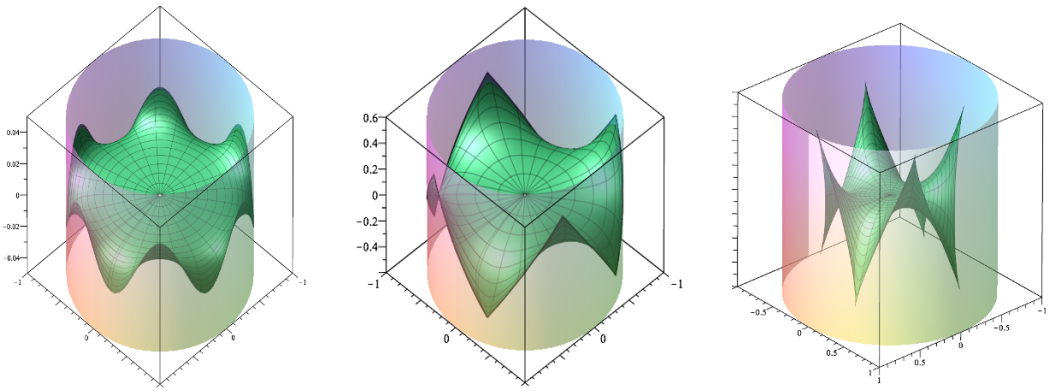

Figure 2. Surface in global coordinates for Lorentzian AdS_3 corresponding to the parameters $[n = 4, \tilde{\alpha}_0 = 0]$, $[n = 2, \tilde{\alpha}_0 = -0.3915941968]$ and $[n = 2, \tilde{\alpha}_0 = -1]$ respectively.

is the same as the one given in the appendix since it does not depend on the signature of space time. The Wilson loop is now given by two real functions $x_\pm(\theta)$. As mentioned, it is convenient to rewrite the contour in terms of

$$\hat{x}_\pm(\theta) = \mp i \frac{1 \pm i x_\pm(\theta)}{1 \mp i x_\pm(\theta)} = e^{i(t \pm \phi)} \,, \tag{6.27}$$

where (t, ϕ) are global coordinates. Notice that $\hat{x}_\pm(\theta)$ have modulus one. In the case of circular Wilson loops, the contour reduces to

$$\hat{x}_\pm(\theta) = e^{\pm i\phi} = e^{\pm i\theta} \,. \tag{6.28}$$

Since the change of variables (6.27) is a global conformal transformation, the Schwarzian derivative with respect to θ is invariant

$$\{\hat{x}_\pm(\theta), \theta\} = \{x_\pm(\theta), \theta\} \,. \tag{6.29}$$

According to the relations [74]

$$\{x_\pm(\theta), \theta\} = \frac{1}{2} - 12\beta_2(\theta) \pm 2f e^{2i\theta} \pm 2\bar{f} e^{-2i\theta} \,, \tag{6.30}$$

we have

$$\begin{aligned} \{\hat{x}_+, \theta\} + \{\hat{x}_-, \theta\} &= 1 - 24\beta_2(\theta) \,, \\ \{\hat{x}_+, \theta\} - \{\hat{x}_-, \theta\} &= 4\,\mathrm{Re}\{e^{2i\theta} f(\theta)\} \,. \end{aligned} \tag{6.31}$$

This is the Minkowski version of (5.7). Using such relations, we can repeat the procedure of minimal area calculation previously done in the Euclidean case, with the cosh-Gordon equation replaced by the sinh-Gordon equation.

The perturbed contour is parametrized as

$$\hat{x}_\pm(\theta) = e^{\pm i s(\theta) + i\epsilon j' \sin(p\, s(\theta))} \,, \tag{6.32}$$

where the i in front of the ϵ is due to the fact that $\hat{x}_\pm(\theta)$ has modulus one.

JHEP08(2016)088

Repeating the calculation, we have

$$
\begin{aligned}
s(\theta) &= \theta + \frac{j'^2(p+5p^3)\sin(2p\theta)}{8(-1+4p^2)}\epsilon^2 + O(\epsilon^4)\,, \\
f(z) &= -\frac{1}{4}j'p\left(p^2-1\right)z^{p-2}\epsilon - \frac{3j'^3p^3\left(p^2-1\right)\left(5p^2+1\right)z^{p-2}}{64\left(4p^2-1\right)}\epsilon^3 + O(\epsilon^4)\,, \\
\alpha(r,\theta) &= \ln\left(\frac{1}{1-r^2}\right) - \frac{j'^2p}{16r^2\left(r^2-1\right)}(4r^2+4r^4-p(p+1)^2r^{2p} \\
&\quad + (p+1)^2(3p-4)r^{2p+2} - (p-1)^2(3p+4)r^{2p+4} + (p-1)^2pr^{2p+6})\epsilon^2 \\
&\quad + O(\epsilon^4)\,.
\end{aligned}
\tag{6.33}
$$

The final result for the area is

$$
\mathcal{A}_f = -2\pi + \frac{1}{2}p\left(p^2-1\right)\pi j'^2\epsilon^2 + \frac{p\left(p^2-1\right)\left(23p^4+p^2\right)\pi j'^4}{32\left(4p^2-1\right)}\epsilon^4 + O(\epsilon^5)\,. \tag{6.34}
$$

The particular contour given by the Mathieu solution is parametrized as

$$
\hat{x}_\pm(\theta) = e^{\pm is(\theta)+i\xi(s(\theta))}\,, \tag{6.35}
$$

where

$$
\xi(s) = jq\sin\left(\frac{s}{\nu}\right) + q^3\left(k\sin\left(\frac{s}{\nu}\right) + l\sin\left(\frac{3s}{\nu}\right)\right)\,. \tag{6.36}
$$

The values of the coefficients are

$$
\begin{aligned}
j &= -\frac{\nu}{\nu^2-1}\,, \\
k &= -\frac{3\nu\left(\nu^2+5\right)}{16\left(\nu^2-4\right)\left(\nu^2-1\right)^3}\,, \\
l &= -\frac{\nu\left(5\nu^4+36\nu^2-89\right)}{48\left(\nu^2-9\right)\left(\nu^2-4\right)\left(\nu^2-1\right)^3}\,.
\end{aligned}
\tag{6.37}
$$

Similar to the Euclidean case, letting $\epsilon = q$, $p = \frac{1}{\nu}$ and making the replacement

$$
j' = j + k\epsilon^2 = -\frac{\nu}{\nu^2-1} - \frac{3\nu\left(\nu^2+5\right)q^2}{16\left(\nu^2-4\right)\left(\nu^2-1\right)^3}\,, \tag{6.38}
$$

in (6.34), we have the area

$$
\mathcal{A}_f = -2\pi + \frac{\pi q^2}{2\nu\left(1-\nu^2\right)} - \frac{\left(5\nu^2+7\right)\pi q^4}{32\nu\left(4-\nu^2\right)\left(1-\nu^2\right)^3} + O(q^5)\,. \tag{6.39}
$$

This result agree with the Mathieu equation calculation and is identical to the result in the Euclidean case. However, now q is real (see eq. (6.11)) and $\mathcal{A}_f > -2\pi$.

JHEP08(2016)088

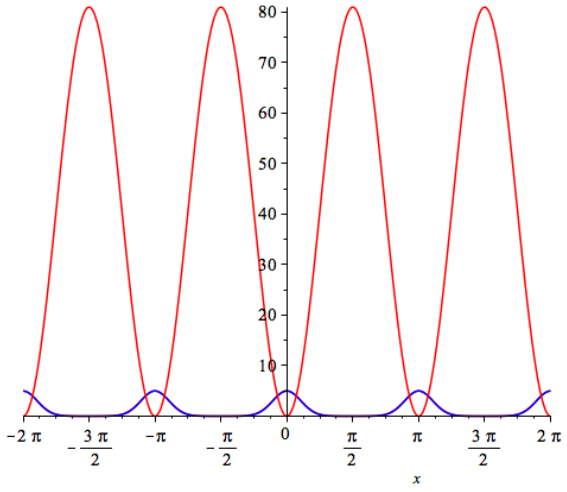

Figure 3. Potential (red) and modulus of the Mathieu function (blue) for $q = 20.25$ and $n = 2$. Clearly the wave-function localizes at the minima.

6.3 Near light-like solution, tight-binding approximation, $q \to \infty$

The Mathieu equation (2.3) can be written as

$$-\partial_u^2\chi + V(u)\chi = a\chi, \qquad V(u) = 2q\cos 2u\,, \tag{6.40}$$

which is a standard Schroedinger equation with potential $V(u)$ and energy a. From eq. (2.7), one can see that the cases $\lambda = e^{i\varphi} = \pm 1$ correspond to $\varphi = 0, \pi$ representing a shift of 0 or $\pi/2$ in u that simply correspond to taking the potential as $V(u)$ or $-V(u)$. Both cases are similar, let us consider first the case $\lambda = -1$ where the potential is $-V(u)$ which is relevant to determine $x_-(s)$ (whereas $+V(u)$ corresponds to x_+). In the limit $q \to \infty$ such potential becomes a set of $n+2$ separated wells, the tunneling between those is suppressed by a potential barrier of height q (and fixed width). The wave function for the ground state is a superposition of localized wave-functions at the different minima. This is clearly seen in figure 3 where the potential and modulus of the Mathieu function are displayed. In this regime, the Mathieu functions can be well approximated by using the tight-binding approximation. It is given by

$$\chi_\nu^{\rm TB}(u) = \sum_{j=-\infty}^{\infty} e^{ij\pi\nu}\,\chi_0(u - j\pi)\,. \tag{6.41}$$

This functions clearly satisfies the periodicity condition $\chi_\nu^{\rm TB}(u+\pi) = e^{i\pi\nu}\chi_\nu^{\rm TB}(u)$ and obeys (approximately) the wave-equation if $\chi_0(u)$ is chosen appropriately. Here we take χ_0 to be a real polynomial times a Gaussian and choose the polynomial such as to minimize the expectation value of the energy. The result is

$$\chi_0(u) = \left(1 + \frac{1}{8}u^2 + \frac{1}{12}\sqrt{q}u^4\right)\, e^{-\sqrt{q}u^2}\,, \tag{6.42}$$

JHEP08(2016)088

with energy given by

$$a_\nu(q) = -2q + 2\sqrt{q} - \frac{1}{4} - \frac{1}{32}\frac{1}{\sqrt{q}} - \frac{3}{256}\frac{1}{q} + \mathcal{O}\left(\frac{1}{q^{3/2}}\right) . \tag{6.43}$$

Notice that in this approximation $a_\nu(q)$ is independent of ν, namely around the given value of $a_\nu(q)$ there is an exponentially small window where ν changes from 0 to 1. An improved result is obtained by replacing the wave function χ_0 away from $u = 0$ by a WKB approximation:

$$\chi_0^{\text{WKB}} = \frac{C}{\kappa(u)} e^{\int^u \kappa(u')du'}, \qquad \kappa(u) = \sqrt{-a(q) - 2q\cos 2u}\,, \tag{6.44}$$

where the constant C is chosen to match the previous approximation $\chi_0(u)$ at some intermediate point.

Since the shape is given by

$$\hat{x}_- = \frac{\left(\chi_\nu^{\text{TB}}\right)^*}{\chi_\nu^{\text{TB}}}\,, \tag{6.45}$$

and the function $\chi_0(u)$ is real, the phase of χ_ν^{TB} changes abruptly when u crosses a maximum of the potential. For example at $u = \frac{\pi}{2}$ in figure 3, the wave function localized around $u = 0$ is replaced by the function localized at $u = \pi$ that is multiplied by a different phase in eq. (6.41). This abrupt changes correspond to the straight lines along x_-. When we consider $\lambda = +1$ the potential is inverted and therefore the minima of the potential correspond to straight lines along x_+. The cusps are associated to the intermediate regions between maxima and minima. In those regions, the phase of χ_ν remains constant implying that $\hat{x}_+$, $\hat{x}_-$ are also constant and equal to their value at the cusp.

It seems possible to define a general procedure to expand around the light-like Wilson loop similar to what can be done around the circle. We leave that for future work. We conclude this part by computing the area in this approximation using eqs. (6.18) and (6.43):

$$\mathcal{A}_f = -2\pi - \frac{\pi}{n+2} + \pi(n+2)\left[-2q + 2\sqrt{q} - \frac{1}{4} - \frac{1}{32}\frac{1}{\sqrt{q}} - \frac{3}{256}\frac{1}{q} + \mathcal{O}\left(\frac{1}{q^{3/2}}\right)\right] . \tag{6.46}$$

When $q \to \infty$ there is a divergence proportional to the number of cusps as we expect from the cusp anomaly computations [50, 57, 75]. Notice that in this limit the number of zeros of $f(z)$ is related to the number of cusps. On the other hand, in the Euclidean case, it does not appear to be such a simple physical interpretation of the number of zeros.

7 Conclusions

One of the most important observables in gauge theories is the Wilson loop. The AdS/CFT correspondence opened up the possibility of studying such operator at strong 't Hooft coupling by using minimal area surfaces. In this paper we consider a previously proposed method to find such surfaces based on the properties of a Schroedinger equation with a potential given by the Schwarzian derivative of the shape of the Wilson loop. It allows us to find new interesting Wilson loops dual to surfaces whose area can be computed analytically

JHEP08(2016)088

in terms of eigenvalues of the Mathieu equation. Those Wilson loops have interesting properties since they can be seen as deformed or regularized versions of previously known solutions: the regular polygons with light-like cusps and also of the multiple wound circular Wilson loop. It also allowed us to check analytically Dekel's method to expand around the circular solutions. Finally, in the near light-like case, we found that the potential becomes a series of separated wells each one associated with a light-like segment. This opens up the possibility of studying systematically perturbations around such Wilson loop, a subject that we leave for future work. Summarizing, we believe that the idea of studying Wilson loops through its associated Schroedinger equation is a productive one that uses the integrability properties of the system and that presumably will lead to further insight into this important operator.

Acknowledgments

We are very grateful to A. Dekel, S. Komatsu, J. Toledo and P. Vieira for useful comments and discussions on this topic. This work was supported in part by DOE through grant DE-SC0007884. M.K. is very grateful to Perimeter Institute for Theoretical Physics for hospitality while this work was being completed.

A Expansion of Mathieu functions

To check the perturbative expansion it is necessary to expand the Mathieu functions for small values of the parameter q appearing in eq. (2.3). More precisely, given $q \ll 1$ and ν, the eigenvalue $a_\nu(q)$ and eigenfunctions χ_ν are expanded as

$$a_\nu(q) = \nu^2 + \sum_{j=1}^{\infty} a_j q^j \,, \tag{A.1}$$

$$\chi_\nu(u) = e^{i\nu u} \sum_{n=-\infty}^{\infty} c_n(q) e^{2inu} \,, \tag{A.2}$$

with the Fourier coefficients c_n expanded as

$$c_n = \sum_{j=1}^{\infty} c_n^{(j)} \, q^j, \qquad (n \neq 0) \,, \tag{A.3}$$

and we take $c_0 = 1$ as a normalization condition. Replacing in the equation a simple recursion relation is obtained that allows an easy computation of the coefficients at any desired order:

$$a_j = c_{-1}^{(j-1)} + c_1^{(j-1)} \,, \tag{A.4}$$

$$c_n^{(j)} = -\frac{1}{4n(n+\nu)} \left[c_{n-1}^{(j-1)} + c_{n+1}^{(j-1)} - \sum_{p=1}^{j-1} a_p c_n^{(j-p)} \right] \,, \tag{A.5}$$

where $n \neq 0$ and $j \geq 1$. These results can then be used in eqs. (2.14) and (3.3) to expand the shape and the area in powers of q. The expansion of the shape is, schematically:

$$X = \frac{\chi_\nu(u)}{\chi_\nu(-u)} = e^{2i\nu u + \chi_1 q \sin 2u + \chi_2 q^2 \sin 4u + \chi_{3a} q^3 \sin 2u + \chi_{3b} q^3 \sin 6u + \mathcal{O}(q^4)}\,, \tag{A.6}$$

where χ_l are constant coefficients. By defining a new variable

$$s = 2\nu u + \chi_2 q^2 \sin 4u + \mathcal{O}(q^4)\,, \tag{A.7}$$

the shape can be written as

$$X = e^{is + \xi(s)}\,, \tag{A.8}$$

where

$$s = 2\nu u - \frac{\nu(\nu^2+5)}{8(\nu^2-1)^2(\nu^2-4)} q^2 \sin 4u + \mathcal{O}(q^4)\,, \tag{A.9}$$

$$\begin{aligned}\xi(s) = {} & \frac{iq\nu}{1-\nu^2}\sin\frac{s}{\nu} - \frac{3}{16}\frac{iq^3\nu(\nu^2+5)}{(\nu^2-1)^3(\nu^2-4)}\sin\frac{s}{\nu} \\ & - \frac{iq^3\nu(5\nu^4+36\nu^2-89)}{48(\nu^2-1)^3(\nu^2-4)(\nu^2-9)}\sin\frac{3s}{\nu} + \mathcal{O}(q^5)\,.\end{aligned} \tag{A.10}$$

Notice that $\xi(s)$ is real since q is purely imaginary (for the Euclidean case). Finally, the area follows from eq. (3.3) as:

$$\begin{aligned}\mathcal{A}_f &= -2\pi + \pi\nu - \frac{\pi}{\nu} a_\nu(q) \\ &= -2\pi + \frac{1}{2}\frac{\pi}{\nu(1-\nu^2)} q^2 - \frac{1}{32}\frac{\pi(5\nu^2+7)}{\nu(4-\nu^2)(1-\nu^2)^3} q^4 + \mathcal{O}(q^6)\end{aligned} \tag{A.11}$$

where we used $\nu = \frac{1}{n+2}$. This result for the area can also be obtained, as done in the main text, by using the shape of the Wilson loop in Dekel's method. The result agrees perfectly providing a useful check.

References

[1] J.M. Maldacena, *The Large-N limit of superconformal field theories and supergravity*, *Int. J. Theor. Phys.* **38** (1999) 1113 [*Adv. Theor. Math. Phys.* **2** (1998) 231] [hep-th/9711200] [INSPIRE].

[2] S.S. Gubser, I.R. Klebanov and A.M. Polyakov, *Gauge theory correlators from noncritical string theory*, *Phys. Lett.* **B 428** (1998) 105 [hep-th/9802109] [INSPIRE].

[3] E. Witten, *Anti-de Sitter space and holography*, *Adv. Theor. Math. Phys.* **2** (1998) 253 [hep-th/9802150] [INSPIRE].

JHEP08(2016)088

[4] G. 't Hooft, *A Planar Diagram Theory for Strong Interactions*, *Nucl. Phys.* **B 72** (1974) 461 [INSPIRE].

[5] G. 't Hooft, *A Two-Dimensional Model for Mesons*, *Nucl. Phys.* **B 75** (1974) 461 [INSPIRE].

[6] J.M. Maldacena, *Wilson loops in large-N field theories*, *Phys. Rev. Lett.* **80** (1998) 4859 [hep-th/9803002] [INSPIRE].

[7] S.-J. Rey and J.-T. Yee, *Macroscopic strings as heavy quarks in large-N gauge theory and anti-de Sitter supergravity*, *Eur. Phys. J.* **C 22** (2001) 379 [hep-th/9803001] [INSPIRE].

[8] D.E. Berenstein, R. Corrado, W. Fischler and J.M. Maldacena, *The Operator product expansion for Wilson loops and surfaces in the large-N limit*, *Phys. Rev.* **D 59** (1999) 105023 [hep-th/9809188] [INSPIRE].

[9] D.J. Gross and H. Ooguri, *Aspects of large-N gauge theory dynamics as seen by string theory*, *Phys. Rev.* **D 58** (1998) 106002 [hep-th/9805129] [INSPIRE].

[10] J.K. Erickson, G.W. Semenoff and K. Zarembo, *Wilson loops in $N = 4$ supersymmetric Yang-Mills theory*, *Nucl. Phys.* **B 582** (2000) 155 [hep-th/0003055] [INSPIRE].

[11] N. Drukker and D.J. Gross, *An Exact prediction of $N = 4$ SUSYM theory for string theory*, *J. Math. Phys.* **42** (2001) 2896 [hep-th/0010274] [INSPIRE].

[12] V. Pestun, *Localization of gauge theory on a four-sphere and supersymmetric Wilson loops*, *Commun. Math. Phys.* **313** (2012) 71 [arXiv:0712.2824] [INSPIRE].

[13] M. Kruczenski and A. Tirziu, *Matching the circular Wilson loop with dual open string solution at 1-loop in strong coupling*, *JHEP* **05** (2008) 064 [arXiv:0803.0315] [INSPIRE].

[14] A. Faraggi and L.A. Pando Zayas, *The Spectrum of Excitations of Holographic Wilson Loops*, *JHEP* **05** (2011) 018 [arXiv:1101.5145] [INSPIRE].

[15] E.I. Buchbinder and A.A. Tseytlin, *$1/N$ correction in the D3-brane description of a circular Wilson loop at strong coupling*, *Phys. Rev.* **D 89** (2014) 126008 [arXiv:1404.4952] [INSPIRE].

[16] V. Forini, V. Giangreco M. Puletti, L. Griguolo, D. Seminara and E. Vescovi, *Precision calculation of 1/4-BPS Wilson loops in $AdS_5 \times S^5$*, *JHEP* **02** (2016) 105 [arXiv:1512.00841] [INSPIRE].

[17] A. Faraggi, L.A. Pando Zayas, G.A. Silva and D. Trancanelli, *Toward precision holography with supersymmetric Wilson loops*, *JHEP* **04** (2016) 053 [arXiv:1601.04708] [INSPIRE].

[18] N. Drukker, D.J. Gross and H. Ooguri, *Wilson loops and minimal surfaces*, *Phys. Rev.* **D 60** (1999) 125006 [hep-th/9904191] [INSPIRE].

[19] N. Drukker, S. Giombi, R. Ricci and D. Trancanelli, *Supersymmetric Wilson loops on S^3*, *JHEP* **05** (2008) 017 [arXiv:0711.3226] [INSPIRE].

[20] N. Drukker and B. Fiol, *On the integrability of Wilson loops in $AdS_5 \times S^5$: Some periodic ansatze*, *JHEP* **01** (2006) 056 [hep-th/0506058] [INSPIRE].

[21] K. Zarembo, *Supersymmetric Wilson loops*, *Nucl. Phys.* **B 643** (2002) 157 [hep-th/0205160] [INSPIRE].

[22] N. Drukker, S. Giombi, R. Ricci and D. Trancanelli, *Supersymmetric Wilson loops on S^3*, *JHEP* **05** (2008) 017 [arXiv:0711.3226] [INSPIRE].

JHEP08(2016)088

[23] N. Drukker, 1/4 *BPS circular loops, unstable world-sheet instantons and the matrix model*, *JHEP* **09** (2006) 004 [hep-th/0605151] [INSPIRE].

[24] B. Fiol and G. Torrents, *Exact results for Wilson loops in arbitrary representations*, *JHEP* **01** (2014) 020 [arXiv:1311.2058] [INSPIRE].

[25] D. Müller, H. Münkler, J. Plefka, J. Pollok and K. Zarembo, *Yangian Symmetry of smooth Wilson Loops in $\mathcal{N} = 4$ super Yang-Mills Theory*, *JHEP* **11** (2013) 081 [arXiv:1309.1676] [INSPIRE].

[26] H. Münkler and J. Pollok, *Minimal surfaces of the $AdS_5 \times S^5$ superstring and the symmetries of super Wilson loops at strong coupling*, *J. Phys.* **A 48** (2015) 365402 [arXiv:1503.07553] [INSPIRE].

[27] S. Ryang, *Algebraic Curves for Long Folded and Circular Winding Strings in $AdS_5 \times S^5$*, *JHEP* **02** (2013) 107 [arXiv:1212.6109] [INSPIRE].

[28] A. Dekel, *Algebraic Curves for Factorized String Solutions*, *JHEP* **04** (2013) 119 [arXiv:1302.0555] [INSPIRE].

[29] A. Dekel and T. Klose, *Correlation Function of Circular Wilson Loops at Strong Coupling*, *JHEP* **11** (2013) 117 [arXiv:1309.3203] [INSPIRE].

[30] A. Irrgang and M. Kruczenski, *Double-helix Wilson loops: Case of two angular momenta*, *JHEP* **12** (2009) 014 [arXiv:0908.3020] [INSPIRE].

[31] V. Forini, V.G.M. Puletti and O. Ohlsson Sax, *The generalized cusp in $AdS_4 \times CP^3$ and more one-loop results from semiclassical strings*, *J. Phys.* **A 46** (2013) 115402 [arXiv:1204.3302] [INSPIRE].

[32] B.A. Burrington and L.A. Pando Zayas, *Phase transitions in Wilson loop correlator from integrability in global AdS*, *Int. J. Mod. Phys.* **A 27** (2012) 1250001 [arXiv:1012.1525] [INSPIRE].

[33] G. Papathanasiou, *Pohlmeyer reduction and Darboux transformations in Euclidean worldsheet AdS_3*, *JHEP* **08** (2012) 105 [arXiv:1203.3460] [INSPIRE].

[34] N. Drukker and V. Forini, *Generalized quark-antiquark potential at weak and strong coupling*, *JHEP* **06** (2011) 131 [arXiv:1105.5144] [INSPIRE].

[35] B.A. Burrington, *General Leznov-Savelev solutions for Pohlmeyer reduced AdS_5 minimal surfaces*, *JHEP* **09** (2011) 002 [arXiv:1105.3227] [INSPIRE].

[36] L.F. Alday and A.A. Tseytlin, *On strong-coupling correlation functions of circular Wilson loops and local operators*, *J. Phys.* **A 44** (2011) 395401 [arXiv:1105.1537] [INSPIRE].

[37] C. Kalousios and D. Young, *Dressed Wilson Loops on S^2*, *Phys. Lett.* **B 702** (2011) 299 [arXiv:1104.3746] [INSPIRE].

[38] R. Ishizeki, M. Kruczenski and A. Tirziu, *New open string solutions in AdS_5*, *Phys. Rev.* **D 77** (2008) 126018 [arXiv:0804.3438] [INSPIRE].

[39] R.A. Janik and P. Laskos-Grabowski, *Surprises in the AdS algebraic curve constructions: Wilson loops and correlation functions*, *Nucl. Phys.* **B 861** (2012) 361 [arXiv:1203.4246] [INSPIRE].

[40] G.W. Semenoff and D. Young, *Wavy Wilson line and AdS/CFT*, *Int. J. Mod. Phys.* **A 20** (2005) 2833 [hep-th/0405288] [INSPIRE].

JHEP08(2016)088

[41] D. Correa, J. Henn, J.M. Maldacena and A. Sever, *An exact formula for the radiation of a moving quark in $N = 4$ super Yang-Mills*, *JHEP* **06** (2012) 048 [arXiv:1202.4455] [INSPIRE].

[42] A. Cagnazzo, *Integrability and Wilson loops: the wavy line contour*, arXiv:1312.6891 [INSPIRE].

[43] A. Dekel, *Wilson Loops and Minimal Surfaces Beyond the Wavy Approximation*, *JHEP* **03** (2015) 085 [arXiv:1501.04202] [INSPIRE].

[44] R. Ishizeki, M. Kruczenski and S. Ziama, *Notes on Euclidean Wilson loops and Riemann theta functions*, *Phys. Rev.* **D 85** (2012) 106004 [arXiv:1104.3567] [INSPIRE].

[45] M. Kruczenski and S. Ziama, *Wilson loops and Riemann theta functions II*, *JHEP* **05** (2014) 037 [arXiv:1311.4950] [INSPIRE].

[46] A. Irrgang and M. Kruczenski, *Rotating Wilson loops and open strings in AdS_3*, *J. Phys.* **A 46** (2013) 075401 [arXiv:1210.2298] [INSPIRE].

[47] M. Babich and A. Bobenko, *Willmore Tori with umbilic lines and minimal surfaces in hyperbolic space*, *Duke Math. J.* **72** (1993) 151.

[48] E.D. Belokolos, A.I. Bobenko, V.Z. Enol'skii, A.R. Its and V.B. Matveev, *Algebro-Geometric Approach to Nonlinear Integrable Equations*, Springer Series in Nonlinear Dynamics, Springer-Verlag, Berlin, Heidelberg and New York (1994).

[49] J.C. Toledo, *Smooth Wilson loops from the continuum limit of null polygons*, arXiv:1410.5896 [INSPIRE].

[50] M. Kruczenski, *A Note on twist two operators in $N = 4$ SYM and Wilson loops in Minkowski signature*, *JHEP* **12** (2002) 024 [hep-th/0210115] [INSPIRE].

[51] L.F. Alday and J.M. Maldacena, *Gluon scattering amplitudes at strong coupling*, *JHEP* **06** (2007) 064 [arXiv:0705.0303] [INSPIRE].

[52] L.F. Alday and J.M. Maldacena, *Comments on gluon scattering amplitudes via AdS/CFT*, *JHEP* **11** (2007) 068 [arXiv:0710.1060] [INSPIRE].

[53] J.M. Maldacena and A. Zhiboedov, *Form factors at strong coupling via a Y-system*, *JHEP* **11** (2010) 104 [arXiv:1009.1139] [INSPIRE].

[54] L.F. Alday, B. Eden, G.P. Korchemsky, J.M. Maldacena and E. Sokatchev, *From correlation functions to Wilson loops*, *JHEP* **09** (2011) 123 [arXiv:1007.3243] [INSPIRE].

[55] L.F. Alday, D. Gaiotto, J.M. Maldacena, A. Sever and P. Vieira, *An Operator Product Expansion for Polygonal null Wilson Loops*, *JHEP* **04** (2011) 088 [arXiv:1006.2788] [INSPIRE].

[56] H. Dorn, N. Drukker, G. Jorjadze and C. Kalousios, *Space-like minimal surfaces in $AdS \times S$*, *JHEP* **04** (2010) 004 [arXiv:0912.3829] [INSPIRE].

[57] L.F. Alday, J.M. Maldacena, A. Sever and P. Vieira, *Y-system for Scattering Amplitudes*, *J. Phys.* **A 43** (2010) 485401 [arXiv:1002.2459] [INSPIRE].

[58] A. Jevicki and K. Jin, *Moduli Dynamics of AdS_3 Strings*, *JHEP* **06** (2009) 064 [arXiv:0903.3389] [INSPIRE].

[59] A. Jevicki, K. Jin, C. Kalousios and A. Volovich, *Generating AdS String Solutions*, *JHEP* **03** (2008) 032 [arXiv:0712.1193] [INSPIRE].

JHEP08(2016)088

[60] M. Kruczenski, *Spin chains and string theory*, *Phys. Rev. Lett.* **93** (2004) 161602 [hep-th/0311203] [INSPIRE].

[61] M. Kruczenski, *Spiky strings and single trace operators in gauge theories*, *JHEP* **08** (2005) 014 [hep-th/0410226] [INSPIRE].

[62] N. Dorey and B. Vicedo, *On the dynamics of finite-gap solutions in classical string theory*, *JHEP* **07** (2006) 014 [hep-th/0601194] [INSPIRE].

[63] K. Sakai and Y. Satoh, *Constant mean curvature surfaces in AdS_3*, *JHEP* **03** (2010) 077 [arXiv:1001.1553] [INSPIRE].

[64] H.J. De Vega and N.G. Sanchez, *Exact integrability of strings in D-Dimensional de Sitter space-time*, *Phys. Rev.* **D 47** (1993) 3394 [INSPIRE].

[65] A.L. Larsen and N.G. Sanchez, sinh-*Gordon,* cosh-*Gordon and Liouville equations for strings and multistrings in constant curvature space-times*, *Phys. Rev.* **D 54** (1996) 2801 [hep-th/9603049] [INSPIRE].

[66] K. Zarembo, *Wilson loop correlator in the AdS/CFT correspondence*, *Phys. Lett.* **B 459** (1999) 527 [hep-th/9904149] [INSPIRE].

[67] K. Pohlmeyer, *Integrable Hamiltonian Systems and Interactions Through Quadratic Constraints*, *Commun. Math. Phys.* **46** (1976) 207 [INSPIRE].

[68] M. Kruczenski, *Wilson loops and minimal area surfaces in hyperbolic space*, *JHEP* **11** (2014) 065 [arXiv:1406.4945] [INSPIRE].

[69] I.S. Gradshteyn and I.M. Ryzhik, *Table of Integrals Series and Products*, A. Jeffrey and D. Zwillinger eds., Academic Press, San Diego CA U.S.A. and London U.K. (2000).

[70] N.W. McLachlan, *Theory and Applications of Mathieu functions*, Clarendon Press, Oxford U.K. (1947).

[71] W. Magnus and S. Winkler, *Hill's Equation*, Dover Books on Mathematics, Dover Publications (2004).

[72] L.F. Alday and J.M. Maldacena, *Null polygonal Wilson loops and minimal surfaces in Anti-de-Sitter space*, *JHEP* **11** (2009) 082 [arXiv:0904.0663] [INSPIRE].

[73] V.Y. Novokshenov, *Minimal surfaces in the hyperbolic space and radial symmetric solutions of the* cosh-*Laplace equation*, INS-251-CLARKSON [INSPIRE].

[74] A. Irrgang and M. Kruczenski, *Euclidean Wilson loops and minimal area surfaces in Lorentzian AdS_3*, *JHEP* **12** (2015) 083 [arXiv:1507.02787] [INSPIRE].

[75] L.F. Alday and J.M. Maldacena, *Gluon scattering amplitudes at strong coupling*, *JHEP* **06** (2007) 064 [arXiv:0705.0303] [INSPIRE].

JHEP08(2016)088